Chapter 3
Preparation of Membranes Based on Polysulfone (PSU) and Graphene Oxide (GrO) by Electrospinning

Yareni Aguilar-Costumbre, Juliette A. Lambert, Miguel A. Meléndez-Lira, and Vladimir A. Escobar-Barrios

3.1 Introduction

Nowadays, more than 700 million people lack access to drinking water sources according to reports of the World Health Organization (WHO) in 2014 [1]. The human water supplies are only 2.5 % of the total of water in the world, with the majority of it located in polar ice caps and glaciers, and just a small portion is surface water [2]. There are several conventional technologies for water purification, such as disinfection, granular filtration, and distillation, among others. In addition, advanced technologies such as membrane filtration, multiple effect distillation, and advanced oxidation process have been recently used for water and wastewater treatment [3]. Desalination technology is based mainly on membranes for the production of drinking water [4, 5] and industrial use. Thus, membrane technology has an important role in the advance of desalination processes and has garnered significant attention in recent years for the development of new materials and production techniques. Nanofibers have been recently used in order to obtain membranes due to their excellent properties such as high surface area to volume ratio, high porosity, and flexibility [6]. The nanofibers can be applied in microfiltration, ultrafiltration, nanofiltration, membrane distillation, and reverse osmosis. This study focuses on evaluating the porosity and diameter of fibers obtained by electrospinning to produce membranes with potential application in filtration process.

Y. Aguilar-Costumbre (✉) • V.A. Escobar-Barrios
Instituto Potosino de Investigación Científica y Tecnológica, Camino a la Presa de San José 2005, Lomas 4 sección, San Luís Potosí, San Luís Potosí 78216, Mexico
e-mail: yareni.aguilar@ipicyt.edu.mx

J.A. Lambert
CIATEC, A.C., Calle Omega 201, Fracc. Industrial Delta, León, Guanajuato 37545, Mexico

M.A. Meléndez-Lira
CINVESTAV-IPN, Av. Instituto Politécnico Nacional 2508, Col. San Pedro Zacatenco, Delegación Gustavo A. Madero, Ciudad de México, DF 07360, Mexico

A. Maciel-Cerda (ed.), *Membranes*, DOI 10.1007/978-3-319-45315-6_3

3.2 Methodology

3.2.1 Materials

Polysulfone (PSU, UDEL-P3500®), Mn = 3.500 g/moL, was provided by Solvay Specialty Polymers; *N*-methyl-pyrrolidone (NMP) by Fisher Scientific (ACS grade); *N*,*N*-dimethyl formamide (DMF) by Fermont (ACS grade); and commercial graphene oxide solution (GrO) by SUPERMARKET (90 nm diameter, 1 nm thickness). All the materials were used as received without any further modification or purification. Only the graphene oxide solution was filtrated and then dried by vacuum desiccator.

3.2.2 Electrospinning

To obtain the membrane, the fibers were processed by electrospinning. First, a polymer solution was prepared by dissolving PSU (20 % w/w) in a solvent mixture of DMF/NMP (30/70 w/w). Then, the PSU was added to the solvent mixture and kept under constant agitation at 60 °C for 24 h, until its dissolution. Finally, 0.15 % wt of dried GrO was added during stirring that continued for additional 15 min.

Electrospinning allowed the formation of fibers through an electric potential difference that was applied to the PSU solution. The high voltage is applied to the PSU solution in order to induce polarization. As a result of such polarization, a Taylor cone is created. When the charge exceeds the surface tension of the solution, a droplet on the tip of the needle (jet) travels towards the region of low potential, in this case the metallic rotary collector.

Figure 3.1 shows the schematic diagram of the electrospinning equipment. It consists of an adjustable DC power supply, which is able to generate a voltage in

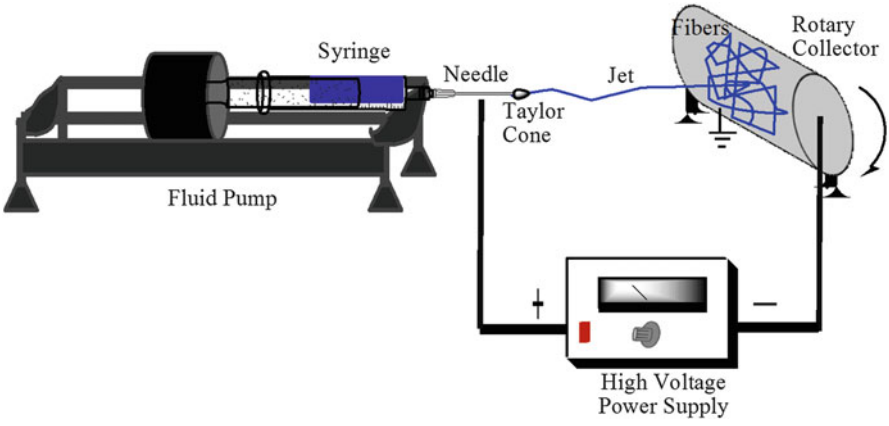

Fig. 3.1 Electrospinning diagram

Table 3.1 Samples obtained by electrospinning

Sample	PSU/GrO (% wt)	Collector-needle distance (cm)	Voltage (kV)	Collector velocity (rpm)	Flow (mL/h)
A	20/0.15	15	20	65	9.8
B	20/0.15	10	25	36	3.42

the range of 0–50 kV. This power supply is connected to a tip of the metallic needle (0.21 mm inner diameter) by two electrodes. The syringe, which contains the polymer solution, is connected to a syringe pump. A positive voltage of 20 or 25 kV was applied across a distance of 10 or 15 cm between the tip of the needle and the metallic collector (17 × 21 cm). The rotary collector was covered with aluminum foil on which the fibers were deposited. The collector velocity was maintained constant at 36 or 65 rpm. Once the membranes were obtained, they were dried in a fume hood for 24 h at room temperature to remove residual solvent. Table 3.1 shows the conditions of the samples obtained.

3.2.3 Membrane Characterization

The morphology of the membranes was studied by scanning electron microscopy (SEM, QUANTA 200, ESEM FEI Co.). Samples of the membranes were gold coated for 25 s, at 40 mA under vacuum conditions, and placed on a pin support. SEM images were analyzed by the ImageJ software in order to determine the diameters and porosity of the obtained fibers. To evaluate the diameter of each sample, three images at the same magnification were considered. Thus, a total number of 200 fibers were measured. In the case of porosity, for each sample the empty area was measured using the contrast difference in the image.

The contact angle of the membrane surface was measured at room temperature by a goniometer (Biolin Scientific, Theta Lite) equipped with the image analysis software One Attention. For this, deionized water drops of about 2.5 μL were placed on the membrane surface using a thin syringe. The contact angle was automatically calculated by the Young–Laplace equation fitting the captured drop shape at both left and right sides of each drop.

The system to carry out the filtration experiments (Amicon 8400, Millipore) has an active membrane area of 0.0045 m^2. It is composed of one cylindrical plastic chamber with the membrane located at the bottom of it; a pure air flow was applied on the top of the chamber. Different operating pressures were considered: 10, 20, 30, and 40 psi. The permeate flux was calculated by measuring the collected volume every 5 min. Finally, the hydraulic resistance was calculated using the Darcy Equation (3.1). The said equation relates the permeate flux J ($m^3/m^2/s$) as a ratio of the difference in pressures ΔP (Pa) (applied pressure and osmotic pressure $\Delta\prod$) and the viscosity μ (kg/m s) and the hydraulic resistance R_H (m^{-1}).

$$J = \frac{\Delta P - \Delta\pi}{\mu R_H} \tag{3.1}$$

The viscosity of water was 0.001002 kg/m^2 s at room temperature and the osmotic pressure was negligible. Cellulose membranes with molecular weight cutoff of 1 and 100 kDa were used as support for every obtained membrane.

3.3 Results and Discussion

3.3.1 Morphology

Figure 3.2 shows the SEM images of the obtained membranes at different voltage, distance, flow, and collector velocity. As it can be seen, the surface exhibits a random arrangement of fibers indicating its chaotic nature (nonwoven).

The variation in the operating conditions affects the fiber diameters. Some studies have reported that fiber diameter depends on polymer concentration; in general, high polymer concentration increases viscosity, and therefore, fibers of larger diameter [7, 8] are obtained. Nevertheless, other groups [9, 10] have reported that voltage plays a more important role in determining the fiber diameters, e.g., when increasing the applied voltage, the electrostatic repulse force would increase the charge on the jet and thus the fiber diameter decreases. The diameter for sample A is 592 nm and sample B is 261 nm; in this case, the applied voltage was higher for sample B, which is according to that reported by Mo [9] and Demir [10]. In addition, the low flow and the collector velocity give a stretched jet polymer and produce

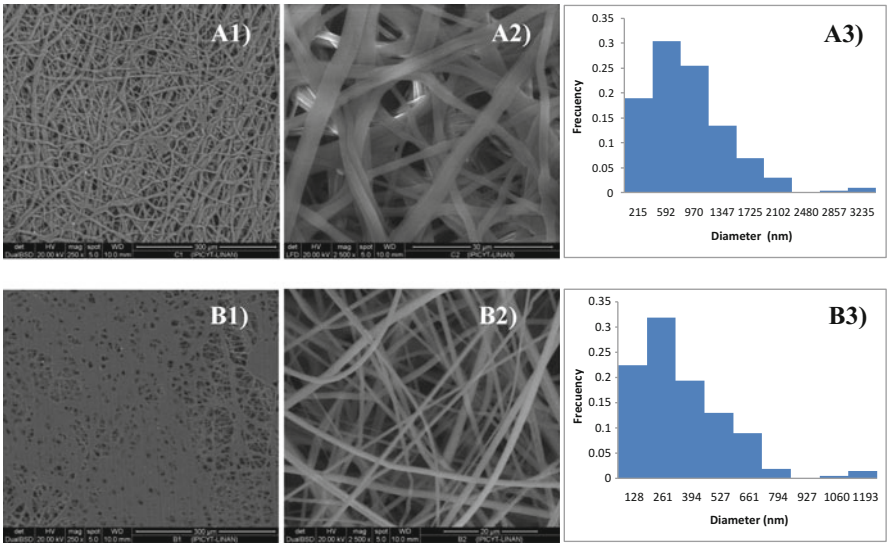

Fig. 3.2 SEM images of (A1) top surface of sample A, (A2) inner fibrous surface of sample A, (A3) diameter distribution of the fibers in A2, (B1) top surface of sample B, (B2) inner fibrous surface of sample B, and (B3) diameter distribution of fibers in B2

fibers of lesser diameters. When the flow was increased, along with the collector velocity, there was not enough time to stretch the polymer jet, and thus the diameter of the fibers increased, as in sample A.

On the other hand, distance plays an important role; sample B (Fig. B2) has a more regular and opened nonwoven membrane unlike sample A (Fig. A2), which has fibers overlapping between them with higher diameters.

The GrO particles were poorly dispersed in the polymer solution; therefore, they are not well dispersed into the fibers. It seems that the presence and distribution of GrO into the fibers have no effect on the morphology of samples A and B.

3.3.2 Hydrophobicity

The hydrophobic nature of the membranes is a function of their chemical composition and rugosity. Polysulfone has a hydrophobic character due to the aromatic ring and the methyl groups, which have no interaction with the water molecules by hydrogen bridges (Fig. 3.3). The method for obtaining the membrane may change the contact angle. For example, the PSU film obtained by phase inversion has a contact angle of 75°, while the film of nonwoven membrane obtained by electrospinning has a contact angle of 135° [9]. This is because the surface area is greater, and there is a higher rugosity in the films formed by the nonwoven fibers.

Figure 3.4 shows the sphericity of the water drops on the surface of samples A and B. As it can be seen, the sphericity is different in both samples. Contact angle values are shown in Table 3.2.

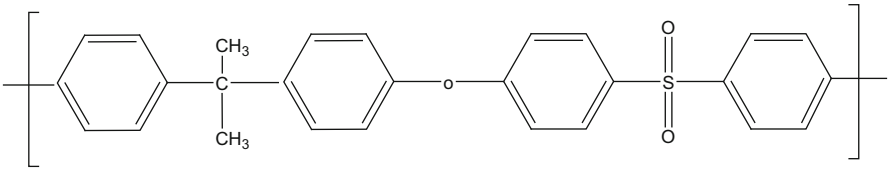

Fig. 3.3 Chemical structure polysulfone (PSU)

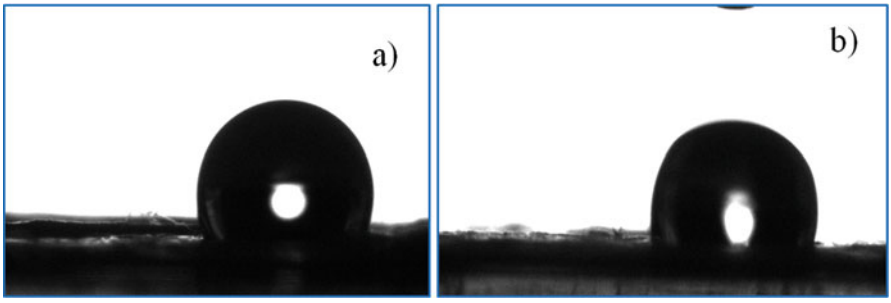

Fig. 3.4 Contact angles of (**a**) membrane A and (**b**) membrane B

Table 3.2 Contact angles of membranes A and B measured with water

	θ_A (°)	θ_B (°)
Mean value	123° ± 2.4	112° ± 6.26

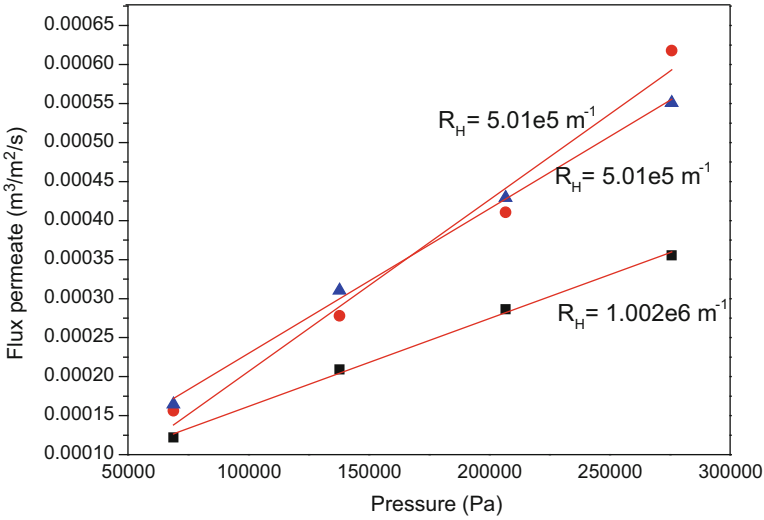

Fig. 3.5 Flux permeate of the membrane in Amicon ultrafiltration 8400 cell; (*black square*) cellulose membrane of 100 kDa; (*red circle*) membrane B with support of 100 kDa; and (*blue triangle*) membrane A with support of 100 kDa

The difference in contact angles is due to the fact that membrane A has a greater contact area due to the overlaps originated in the electrospinning process. Larger diameters of fibers mean a greater contact area and therefore a greater contact angle. Membrane B presents a more randomized distribution of fibers of smaller diameters but with larger interfiber spaces.

3.3.3 Test Filtration

Membranes were evaluated using commercial cellulose membranes (Millipore) as support. Such supporting membranes have a molecular weight cutoff of 100 and 1 kDa, and they were used in order to avoid ruptures of the obtained PSU membranes with low mechanical strength. The tests were carried out at pressures of 10, 20, 30, and 40 psi at room temperature. Figure 3.5 shows the obtained results.

From Fig. 3.5, it is observable that both membranes, A and B, show a similar behavior with no apparent significant difference between them regarding the permeated flow. Therefore, the hydraulic resistance between the two membranes is very similar. However, in Fig. 3.6, it can be seen that membrane B shows a

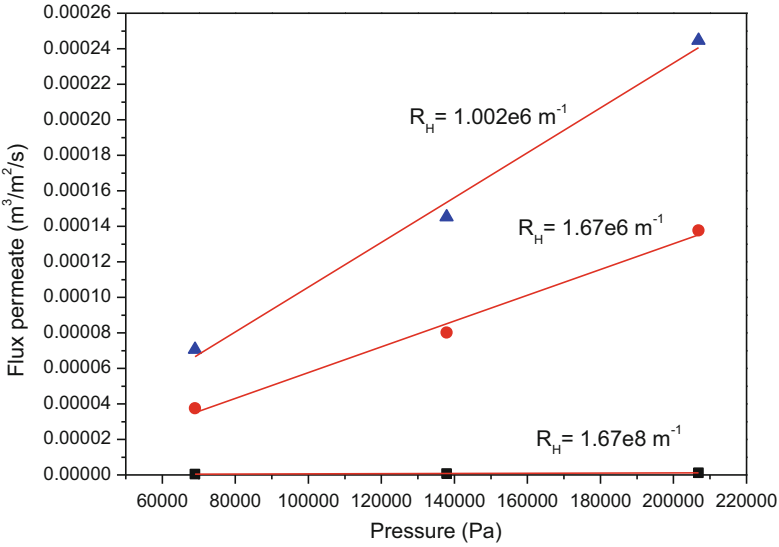

Fig. 3.6 Flux permeate of the membrane in Amicon ultrafiltration 8400 cell; (*black square*) cellulose membrane of 1 kDa; (*red circle*) membrane B with support of 1 kDa; and (*blue triangle*) membrane A with support of 1 kDa

Table 3.3 Porosity of membrane obtained by electrospinning

Sample	Average size	% Area
A	266	65.07
B	135.71	51.27

hydraulic resistance of 16.7e5m^{-1}, which is 43 % greater than the value for the membrane A (10.2e5m^{-1}). Thus, membrane B would have a better performance in water treatment system. The difference between them could be attributed to the differences in porosity.

The average size and porosity (% area) are reported in Table 3.3 below.

Table 3.3 shows a slight difference in porosity; however, in terms of average size, sample B has a value of half of that for sample A. Thus, the hydraulic resistance is higher in sample B than in sample A.

3.4 Conclusions

It is possible to obtain hydrophobic membranes by electrospinning with different hydraulic resistances. The synthesis conditions influence the characteristics of the obtained membranes. As the flow and the distance are decreased and voltage is higher, the fiber diameters are more homogeneous and have a better distribution in the membrane. The membranes exhibited a hydrophobic character due to polysulfone, and the graphene oxide did not have a noticeable effect on the obtained membranes since it

was not properly dispersed into them. The membrane with lower porosity showed a high hydraulic resistance.

It seems that the obtained membranes could be used in the distillation by membrane process due to its hydrophobic nature, high flow, hydraulic resistance, and low membrane thickness.

References

1. WHO-UNICEF. (2014). WHO Library Cataloguing-in-Publication Data, p. 6.
2. UNESCO, WMO, IAEA. (2006). World Water Assessment Programme, p. 4.
3. Shannon, M. A., Bohn, P. W., Elimelech, M., Georgiadis, J. G., Mariñas, B. J., & Mayes, A. M. (2008). Science and technology for water purification in the coming decades. *Nature, 452*, 301–310.
4. Khawaji, A. D., Kutubkhanah, I. K., & Wie, J. M. (2008). Advances in seawater desalination technologies. *Desalination, 221*, 47–69.
5. Lawson, K. W., & Loyd, D. R. (1997). Membrane distillation. *Journal of Membrane Science, 124*, 1–25.
6. Ahmed, F. E., Lalia, B. S., & Hashaikeh, R. (2015). A review on electrospinning for membrane fabrication: Challenges and applications. *Desalination, 356*, 15–30.
7. Ma, Z., Kotaki, M., & Ramakrishna, S. J. (2006). Surface modified nonwoven polysulphone (PSU) fiber mesh by electrospinning: A novel affinity membrane. *Journal of Membrane Science, 272*, 179–187.
8. Essalhi, M., & Khayet, M. (2014). Self-sustained webs of polyvinylidene fluoride electrospun nano-fibers: Effects of polymer concentration and desalination by direct contact membrane distillation. *Journal of Membrane Science, 454*, 133–143.
9. Mo, X. M., Xu, C. Y., Kotaki, M., & Ramakrishna, S. (2004). Electrospun P(LLA-CL) nanofiber: A biomimetic extracellular matrix for smooth muscle cell and endothelial cell proliferation. *Biomaterials, 25*, 1883–1890.
10. Demir, M. M., Yilgor, I., Yilgor, E. E. A., & Erman, B. (2002). Electrospinning of polyurethane fibers. *Polymer, 43*, 3303–3309.